The Journal of Immunology

RESEARCH ARTICLE | JULY 01 2010

Myeloid PTEN Promotes Inflammation but Impairs Bactericidal Activities during Murine Pneumococcal Pneumonia

Gernot Schabbauer; ... et. al

J Immunol (2010) 185 (1): 468–476.
https://doi.org/10.4049/jimmunol.0902221

Myeloid PTEN Promotes Inflammation but Impairs Bactericidal Activities during Murine Pneumococcal Pneumonia

Gernot Schabbauer,*[,1] Ulrich Matt,[†,1] Philipp Günzl,* Joanna Warszawska,[†,‡] Tanja Furtner,[†,‡] Eva Hainzl,* Immanuel Elbau,[†,‡] Ildiko Mesteri,[§] Bianca Doninger,[†] Bernd R. Binder,* and Sylvia Knapp[†,‡]

Phosphatidylinositol 3-kinase has been described as an essential signaling component involved in the chemotactic cell influx that is required to eliminate pathogens. At the same time, PI3K was reported to modulate the immune response, thus limiting the magnitude of acute inflammation. The precise role of the PI3K pathway and its endogenous antagonist phosphatase and tensin homolog deleted on chromosome 10 (PTEN) during clinically relevant bacterial infections is still poorly understood. Utilizing mice lacking myeloid cell-specific PTEN, we studied the impact of PTEN on the immune response to *Streptococcus pneumoniae*. Survival analysis disclosed that PTEN-deficient mice displayed less severe signs of disease and prolonged survival. The inflammatory response to *S. pneumoniae* was greatly reduced in macrophages in vitro and in vivo. Unexpectedly, neutrophil influx to the lungs was significantly impaired in animals lacking myeloid-cell PTEN, whereas the additional observation of improved phagocytosis by alveolar macrophages lacking PTEN ultimately resulted in unaltered lung CFUs following bacterial infection. Together, the absence of myeloid cell-associated PTEN and consecutively enhanced PI3K activity dampened pulmonary inflammation, reduced neutrophil influx, and augmented phagocytic properties of macrophages, which ultimately resulted in decreased tissue injury and improved survival during murine pneumococcal pneumonia. *The Journal of Immunology*, 2010, 185: 468–476.

Infectious diseases are a major burden for our society, with respiratory tract infections being a leading cause of morbidity and mortality worldwide. *Streptococcus pneumoniae* is the most frequent causative pathogen of community acquired pneumonia, affecting >500,000 people in the United States annually (1, 2). The worldwide increase in antibiotic resistance among *S. pneumoniae* strains underlines the urgent need for a better understanding of molecular mechanisms associated with pneumococcal pneumonia (3).

The phosphatase and tensin homolog deleted on chromosome 10 (PTEN) is a well-described tumor suppressor gene and multifunctional phosphatase that antagonizes PI3K's enzymatic activity by dephosphorylating phosphatidylinositol (3,5)-trisphosphate to generate phosphatidylinositol (4,5)-biphosphate. PI3K's enzymatic activity is warranted by two distinct subclasses, namely class Ia (p110α, β, δ) and class Ib (p110γ) (4). PTEN efficiently limits PI3K activity and downstream Akt signaling. PI3K/PTEN has been shown to play a prominent role in a variety of cellular mechanisms, such as survival, migration, and proliferation (5). However, little is known about the biological role of PTEN in inflammation and in particular during infectious diseases. The PI3K/Akt signaling axis is crucial for site-directed migration and diapedesis of immune effector cells, such as neutrophils and monocytes, to the site of inflammation and infection (6–10). In contrast to the conception that PI3K mediates proinflammatory signals, several studies indicate that the PI3K/PTEN pathway modulates the inflammatory response to bacterial cell wall components (11–15). Making use of a combination of pharmacologic and genetic means, we and others could previously show that the PI3K pathway provides beneficial anti-inflammatory properties in mouse models of endotoxemia and sepsis. These observations have been further supported by Martin et al. (16), who intriguingly demonstrated that TLR-induced PI3K/Akt activation phosphorylated, and thereby inactivated, downstream glycogen synthase kinase (GSK) 3β, which in turn resulted in diminished NF-κB–driven proinflammatory gene expression in monocytic cells.

The precise function of PI3K signaling during infections with viable bacteria is less well understood. Maus et al. (17) published a report that investigated the contribution of the γ-catalytic subunit of PI3K (p110γ) during pneumococcal pneumonia. They hereby demonstrated that p110γ, which is generally thought to be responsible for the G-protein coupled receptor-induced chemotactic response of neutrophils and monocytes, was not required for neutrophil influx

*Department of Vascular Biology and Thrombosis Research, Center for Biomolecular Medicine and Pharmacology, [‡]Division of Infectious Diseases and Tropical Medicine, Department of Medicine I, and [§]Institute for Clinical Pathology, Medical University of Vienna, Wien; and [†]Research Center for Molecular Medicine, Austrian Academy of Sciences, Vienna, Austria

[1]G.S. and U.M. contributed equally to this work.

Received for publication July 9, 2009. Accepted for publication April 22, 2010.

This work was supported in part by Grant FWF P19850-B12 from the Austrian Science Fund (to G.S.).

Address correspondence and reprint requests to Dr. Gernot Schabbauer, Department of Vascular Biology and Thrombosis Research, Center for Biomolecular Medicine and Pharmacology, Medical University of Vienna, Schwarzspanierstrasse 17, 1090 Wien, Austria, or Dr. Sylvia Knapp, Center for Molecular Medicine of the Austrian Academy of Sciences, Division of Infectious Diseases and Tropical Medicine, Department of Medicine I, Medical University of Vienna, Waehringer Guertel 18-20, 1090 Vienna, Austria. E-mail addresses: gernot.schabbauer@meduniwien.ac.at or sylvia.knapp@meduniwien.ac.at

Abbreviations used in this paper: AM, alveolar macrophage; BAL, bronchoalveolar lavage; BALF, bronchoalveolar lavage fluid; BMDM, bone marrow-derived macrophage; GSK, glycogen synthase kinase; iNOS, inducible NO synthase; KC, keratinocyte-derived chemokine; LysM, lysozyme M; MPO, myeloperoxidase; PTEN, phosphatase and tensin homolog deleted on chromosome 10.

following pulmonary inoculation of pneumolysin or whole bacteria in vivo (17). However, p110γ-deficient mice displayed an impaired bacterial clearance and delayed recruitment of exudate macrophages (17).

Still, the role of myeloid cell-associated PTEN upon infection with clinically relevant pathogens in healthy mice, such as community-acquired pneumonia by *S. pneumoniae*, is incompletely understood. The increasing number of patients and clinical trials applying drugs targeting the PI3K/PTEN pathway highlights the urgent need for better comprehension of PI3K/PTEN signaling during clinically relevant infections (18). To elucidate the contribution of myeloid cell-associated PI3K/PTEN during *S. pneumoniae* infection, we therefore made use of a conditional knockout strategy to specifically eliminate PTEN expression in myeloid cells (we hereafter refer to these mice as $PTEN^{MC\text{-}KO}$ animals and $PTEN^{MC\text{-}Wt}$ littermate controls, respectively). Pneumococcal pneumonia was then induced in $PTEN^{MC\text{-}KO}$ mice, which displayed enhanced PI3K activity, and littermate $PTEN^{MC\text{-}Wt}$ controls, after which the inflammatory response was investigated.

Materials and Methods

Mice

Floxed PTEN mice were kindly provided by T.W. Mak (Cancer Institute at Princess Margaret Hospital, University Health Network, Toronto, Ontario, Canada) (19); lysozyme M (LysM) Cre recombinase transgenic mice were a kind gift from R. Johnson (University of California San Diego, La Jolla, CA) (20). PI3Kγ (p110γ) mice were obtained from J.M. Penninger (Institute of Molecular Biotechnology of Austrian Academy of Sciences, Vienna, Austria) (9). Intercrossed mice were backcrossed to a C57BL/6J background for at least eight generations. Littermate-controlled experiments were performed using 8–12-wk-old male mice. For genotyping, murine tissue was lysed in PCR-lysis buffer, and direct PCR was performed using GoTaq DNA Polymerase (Promega, Madison, WI). All animal studies were approved and comply with institutional guidelines (BMWF-66.009/0103-C/GT/2007).

Harvest of primary cells

Thioglycollate-elicited peritoneal macrophages were isolated from $PTEN^{MC\text{-}KO}$ and $PTEN^{MC\text{-}Wt}$ controls as described previously (21). Alveolar macrophages were isolated by bilateral bronchoalveolar lavage (BAL) as described elsewhere (22, 23). Bone marrow was isolated from femurs and tibias of healthy $PTEN^{MC\text{-}KO}$ and $PTEN^{MC\text{-}Wt}$ mice. Bone marrow cells were incubated with conditioned media from L929 cells (20% in RPMI 1640) for 10 d to allow differentiation and maturation of macrophages.

Western blotting

Macrophage cell lysates were separated by SDS-PAGE, blotted to membrane (Immobilon PVDF Transfer Membrane, Millipore, Bedford, MA), probed with rabbit primary Abs against PTEN, protein kinase B, phospho-protein kinase B (Ser473), phospho-GSK3β (Ser9) (Cell Signaling Technology, Beverly, MA), and β-actin (Sigma-Aldrich, St. Louis, MO). For detection, a goat anti-rabbit secondary Ab conjugated with HRP (Amersham Biosciences, Piscataway, NJ) was used.

Inducible NO synthase induction and NO generation assay

RNA from cell culture was extracted using Qiagen's RNEasy kit (Qiagen, Valencia, CA), and real-time PCR was conducted according to the LightCycler FastStart DNA MasterPLUS SYBR Green I system using the Roche Light cycler II sequence detector (Roche Diagnostic Systems, Somerville, NJ). Cycling conditions were set at 1 cycle at 95°C for 10 min, 50 cycles at 95°C for 5 s, 68°C for 5 s, and 72°C for 10 s. To confirm specificity of the reaction products, the melting profile of each sample was analyzed using the LightCycler Software 3.5 (Roche Diagnostic Systems). Mouse gene-specific primer sequences for inducible NO synthase (iNOS) were: 5′-ACC TCA CTG TGG CCT TGG TC-3′ (forward) and 5′-GGG TCC TCA GGG AGC TGG AA-3′ (reverse). NO release was measured by the generation of nitrite (Sigma-Aldrich) in supernatants of $PTEN^{MC\text{-}KO}$ and $PTEN^{MC\text{-}Wt}$ littermate control macrophages incubated with heat-killed *S. pneumonia* (ATCC 6303) for 24 h. Assays were performed according to the manufacturer's protocol (24).

Phagocytosis and killing assays

Primary alveolar macrophages (AMs) were incubated with FITC-labeled heat-killed *S. pneumoniae* (ATCC 6303) at a multiplicity of infection of 100 for 30 min at 37°C. After washing steps, lysosomes were stained with Lysotracker red and nuclei with DAPI (Invitrogen, Carlsbad, CA), followed by visualization using confocal laser scanning microscopy (LSM 510, Zeiss, Oberkochen, Germany). The ratio of engulfed bacteria (as determined by overlay of green bacteria and red lysosomes) were quantified by an independent researcher from 300–400 counted cells per well and are expressed as percentage of cells that contain bacteria. In addition, an FACS-based phagocytosis assay was performed exactly as described earlier (25). In brief, primary AMs were allowed to adhere overnight before being incubated with FITC-labeled *S. pneumoniae* at 37°C or 4°C, respectively. Uptake of bacteria was quantified by FACS, and the phagocytosis index was calculated as follows: (mean fluorescence × % positive cells at 37°C) − (mean fluorescence × % positive cells at 4°C). Bacterial killing was performed as described (25). In brief, AMs were isolated, plated at a density of 2×10^5 cells/well, and allowed to adhere. *S. pneumoniae* were added at a multiplicity of infection of 100, and plates were placed at 37°C for 10 min. Each well was then washed five times with ice-cold PBS to remove extracellular bacteria. To determine bacterial uptake after 10 min, triplicate of wells were lysed with sterile H_2O and designated as $t = 0$. Prewarmed SF-RPMI 1640 was added to remaining wells, and plates were

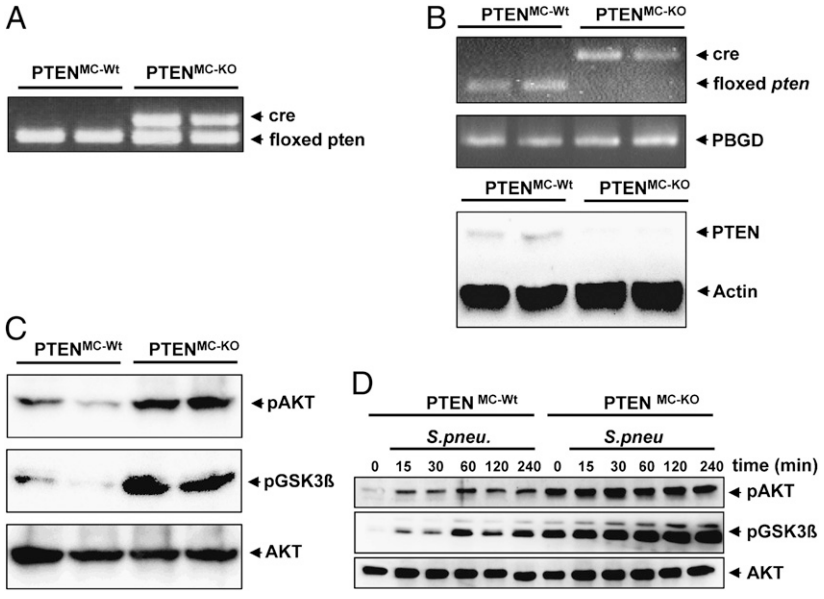

FIGURE 1. PTEN deficiency in myeloid cells. *A*, Genomic DNA PCR analysis of *pten* and *cre* alleles was performed on tissue from fl/fl *pten*, LysM Cre-positive, or -negative mice. *B*, Excision of the *pten* allele was detected by PCR analysis of macrophage genomic DNA; *pbgd* was used as internal control. PTEN deficiency of peritoneal macrophages was analyzed by Western blotting using a PTEN-specific Ab. Cell lysates derived from two mice per genotype are shown. *C*, Constitutive PI3K/PTEN-dependent signaling was determined in resting macrophages derived from two mice per genotype using phospho-Akt and phospho-GSK3β Abs. Total Akt was used as loading control. *D*, Time course analysis of PI3K/PTEN-dependent signaling in *S. pneumoniae*-stimulated macrophages. Phosphorylation of Akt and GSK3β was determined by Western blotting. Total Akt was used as loading control.

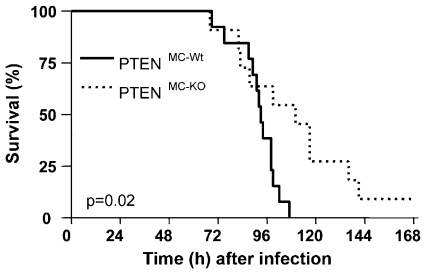

FIGURE 2. Improved survival of pneumococci infected PTEN$^{MC\text{-}KO}$ mice. PTEN$^{MC\text{-}KO}$ and PTEN$^{MC\text{-}Wt}$ littermate controls were infected intranasally with *S. pneumoniae* (4×10^5 CFU) and monitored over 7 d (n = 11–13 per group). Statistical analysis was performed by log-rank test; the p value is depicted in the graph.

placed at 37°C for 10, 30, 60, or 90 min, after which cells were again washed five times with ice-cold PBS and lysed as described above. Cell lysates were plated in serial-fold dilutions on blood agar plates, and bacterial counts were enumerated after 16 h. Bacterial killing was expressed as the percentage of killed bacteria in relation to $t = 0$ (percent killing = 100 − [(number of CFUs at time x/number of CFUs at time 0) × 100]).

Pneumonia experiments

Pneumococcal pneumonia was induced as described previously (26–28). Briefly, *S. pneumoniae* serotype 3 was obtained from American Type Culture Collection (ATCC 6303, Rockville, MD) and grown to log-phase. Mice were short-term anesthetized with isoflurane (Forene, Abbott Laboratories, Abbott Part, IL) and 50 μl bacterial suspension (~5×10^4 CFUs) was inoculated intranasally. For survival analysis, infected mice were observed every 3 h. At indicated time points, mice were sacrificed; BAL was performed, and blood and lungs were collected and processed as described (27, 29). CFUs were determined from serial dilutions of lung homogenates, blood, and BAL fluid (BALF), plated on blood agar plates, and incubated at 37°C for 16 h before colonies were counted. Cytokines and chemokines were quantified in lung homogenates and BALF. TNF-α, IL-6, keratinocyte-derived chemokine (KC), MCP-1, and MIP-2 were measured using ELISAs (R&D Systems, Minneapolis, MN), as was myeloperoxidase (MPO) (HyCult Biotechnology, Uden, The Netherlands) and IL-10 (Bender Medsystems, Vienna, Austria). Detection limits were: 15 ng/ml for TNF-α; 16 pg/ml for IL-6; 12 pg/ml for KC; 4 pg/ml for MCP-1; 94 pg/ml for MIP-2; and 15 pg/ml for IL-10. Differential cell counts were determined using counting chambers and cytospin preparations stained with Giemsa.

Histology

Lungs were fixed in formalin and embedded in paraffin; 4-μm sections were stained in H&E and analyzed by a blinded pathologist. The lung was scored with respect to the following parameters: interstitial inflammation, edema, endothelitis, bronchitis, pleuritis, and thrombi formation. Each parameter was graded on a scale of 0–3 (0: absent; 1: mild; 2: moderate; and 3: severe). The total lung inflammation score was expressed as the sum of the scores for each parameter, the maximum being 18. Granulocyte immunostaining was performed on paraffin-embedded lungs as described (27). After Ag retrieval using pepsin, tissue sections were incubated with FITC rat anti-mouse Ly-6G (BD Biosciences, San Jose, CA) or corresponding isotype control IgG (Emfret Analytics, Würzburg, Germany), followed by rabbit anti-FITC Ab (Zymed, Invitrogen) in normal mouse serum. Finally, slides were incubated with polyclonal anti-rabbit-HRP Ab (Immunologic, Duiven, The Netherlands) and visualized using 3,3-diaminobenzidine-tetrahydrochloride (Vector Laboratories, Burlingame, CA). Counterstaining was done with hemalaun solution.

Statistical analysis

Data were analyzed with GraphPad Prism 4 software (GraphPad, San Diego, CA) using unpaired Student t test or one-way ANOVA followed by post hoc tests when appropriate. Bacterial killing data were calculated by two-way ANOVA. Survival data were analyzed by Kaplan-Meier followed by log-rank test. Criteria for significance for all experiments were $p < 0.05$.

Results

PTEN depletion is associated with enhanced PI3K activity in macrophages

To investigate the role of myeloid cell-derived PTEN during the inflammatory response to bacterial infections, we generated conditional *pten* knockout mice in which PTEN expression was controlled by *LysM*, a myeloid cell-specific promoter (20). Depending on the presence of LysM Cre recombinase, double-floxed (*pten*$^{flox/flox}$) mice are referred to as PTEN$^{MC\text{-}KO}$ or PTEN$^{MC\text{-}Wt}$ mice, respectively (Fig. 1*A*). Deletion of PTEN was confirmed in primary macrophages (Fig. 1*B*), and resulting downstream effects of constitutively active PI3K were reflected by greatly elevated baseline levels of phospho-Akt and phospho-GSK3β in PTEN$^{MC\text{-}KO}$ macrophages (Fig. 1*C*). These findings also indicate that alternative

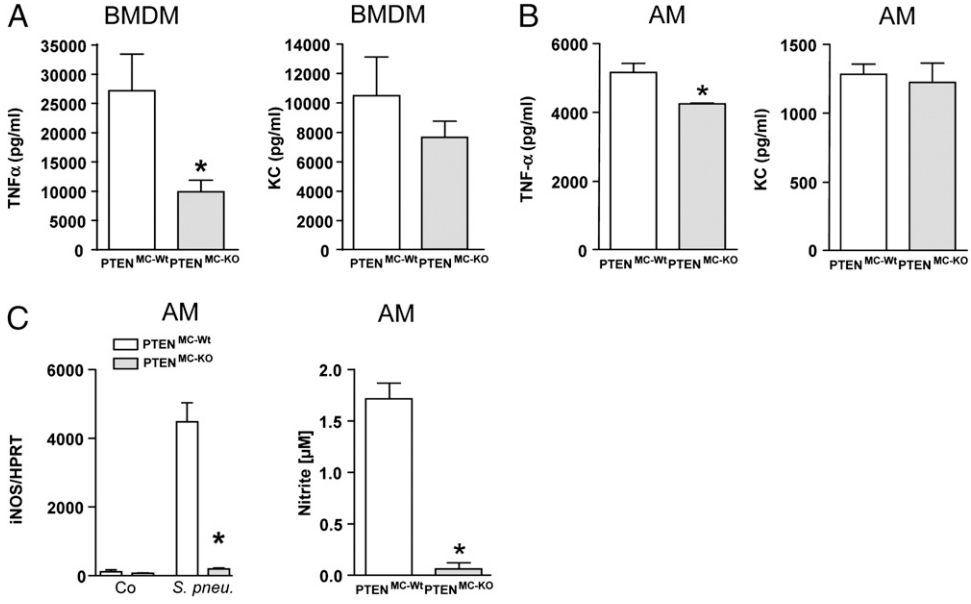

FIGURE 3. Role of PTEN in inflammation in vitro. BMDMs (*A*) and AMs (*B*, *C*) were stimulated with *S. pneumoniae* (10^7 CFU/ml) for 6 h, and TNF-α and KC release was measured in supernatants (*A*, *B*). *C*, iNOS expression was assessed by RT-PCR, and NO release was quantified in supernatants (t = 16 h). Data are representative of two independent experiments and show mean ± SEM of n = 3/genotype for BMDM and n = 4/genotype for AM. $*p < 0.05$ versus PTEN$^{MC\text{-}Wt}$.

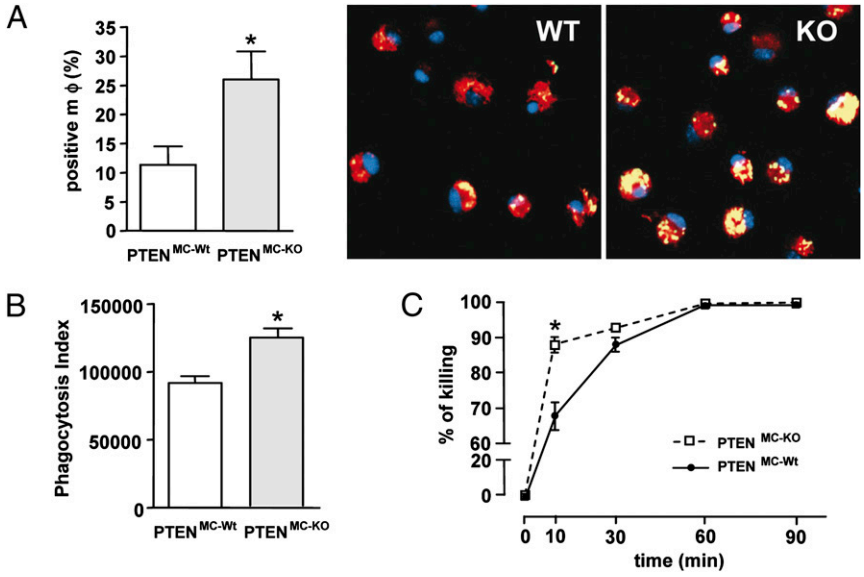

FIGURE 4. Role of PTEN in bacterial uptake and killing by AMs. AMs from PTEN$^{MC\text{-}KO}$ and PTEN$^{MC\text{-}Wt}$ littermate control mice were incubated with FITC-labeled *S. pneumoniae* for 30 min, and uptake of bacteria was quantified by microscopy (*A*) or FACS (*B*) as described in the *Materials and Methods*. *A*, The percentage of macrophages that contained bacteria and representative confocal microscopy images of AM ($n = 3$ per genotype) are depicted: PTEN$^{MC\text{-}Wt}$ (*left panel*) and PTEN$^{MC\text{-}KO}$ (*right panel*). Original magnification ×100. Nuclei are stained with DAPI (blue); ingested bacteria (green) are defined by colocalization with lysosomes (red) and appear yellow. *B*, Phagocytosis of bacteria was analyzed by FACS. *C*, Time-dependent bacterial killing by AM was analyzed as described in the *Materials and Methods* section. Data are presented as mean ± SEM. $*p < 0.05$ versus PTEN$^{MC\text{-}Wt}$.

lipid phosphatases, such as SHIP1 and SHIP2, which are known to influence phosphatidylinositol (3,4,5)-triphosphate plasma membrane content (30), do not sufficiently limit PI3K activity in macrophages or compensate for the loss of PTEN.

To characterize PTEN-associated properties of macrophages during bacterial infection, we next examined kinase phosphorylation downstream of PI3K in PTEN$^{MC\text{-}Wt}$ and PTEN$^{MC\text{-}KO}$ macrophages upon stimulation with *S. pneumoniae*. Bacterial challenge led to Akt and GSK3β phosphorylation in PTEN$^{MC\text{-}Wt}$ cells with highest levels 60 min postactivation (Fig. 1*D*). Although Akt phosphorylation only modestly increased over baseline levels upon *S. pneumoniae* stimulation in PTEN-deficient macrophages, GSK3β phosphorylation was found markedly enhanced in these cells (Fig. 1*D*). These data illustrate that the innate immune response to *S. pneumoniae* involves downstream PI3K pathway activation.

Improved survival of PTEN$^{MC\text{-}KO}$ mice infected with S. pneumoniae

To test whether PTEN deficiency in myeloid cells might impact the outcome of pneumococcal pneumonia in vivo, we infected PTEN$^{MC\text{-}KO}$ and PTEN$^{MC\text{-}Wt}$ mice with 5×10^4 CFU *S. pneumoniae* and monitored survival over 7 d. Already 2 d postinfection, we found PTEN$^{MC\text{-}KO}$ mice to show less severe signs of disease, which was quantified using a clinical severity score (data not shown). PTEN$^{MC\text{-}Wt}$ animals rapidly displayed signs of serious infection, and all mice succumbed within 107 h postinduction of pneumonia,

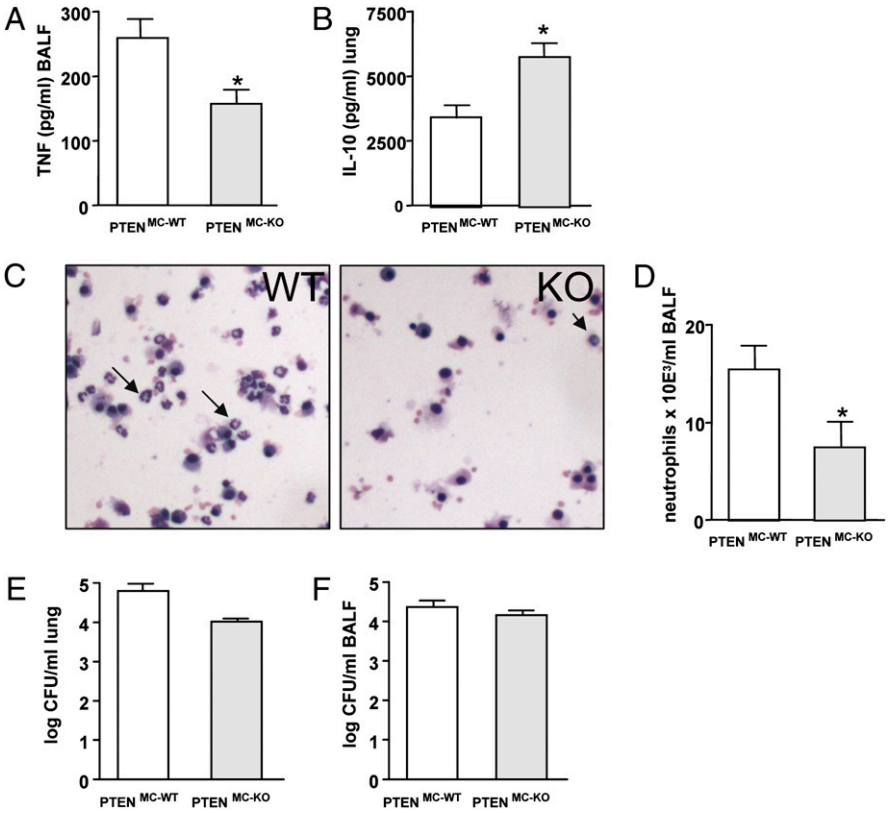

FIGURE 5. Role of PTEN early post-induction of pneumonia (6 h). PTEN$^{MC\text{-}KO}$ and PTEN$^{MC\text{-}Wt}$ mice were infected intranasally with *S. pneumoniae* (4×10^5 CFU); BALF and lungs were harvested 6 h postinfection. TNF-α levels in BALF (*A*) and lung IL-10 concentrations (*B*) were determined by ELISA. Representative BALF cytospins stained with Giemsa are depicted in *C* (neutrophils are indicated by arrows; original magnification ×20). Enumeration of neutrophils in BALF (*D*). Bacterial CFU counts were determined in lung homogenates (*E*) and BALF (*F*). Data are presented as mean ± SEM of $n = 6$–7 mice/group. $*p < 0.05$.

Table I. *BALF cytokine and chemokine levels (pg/ml) in PTEN$^{MC\text{-}KO}$ and PTEN$^{MC\text{-}Wt}$ mice 48 h post* S. pneumoniae *infection*

BALF	PTEN$^{MC\text{-}Wt}$	PTEN$^{MC\text{-}KO}$
TNF-α	1566 ± 586	206 ± 60*
IL-6	379 ± 191	104 ± 15
KC	162 ± 41	85 ± 18*
MCP-1	929 ± 393	229 ± 128*

Data are presented as mean ± SEM of n = 9–10 mice/group.
*$p < 0.05$.

at a time when >50% of PTEN$^{MC\text{-}KO}$ animals were still alive (Fig. 2). Together, myeloid-cell specific PTEN deficiency was associated with less severe signs of disease and significantly improved survival during pneumococcal pneumonia in vivo.

PTEN enhanced the inflammatory response and attenuated bactericidal properties in vitro

In our effort to elucidate the detrimental role of PTEN during pneumococcal pneumonia, we investigated PTEN's contribution to basic functional properties of myeloid cells, such as cytokine secretion or bacterial phagocytosis and killing. Upon stimulation of bone marrow-derived macrophages (BMDMs) and primary AMs from PTEN$^{MC\text{-}KO}$ and PTEN$^{MC\text{-}Wt}$ mice with *S. pneumoniae*, we observed a significantly reduced TNF-α release by PTEN$^{MC\text{-}KO}$ macrophages compared with PTEN$^{MC\text{-}Wt}$ cells, whereas KC levels did not differ significantly (Fig. 3*A*, 3*B*). To study effector molecules importantly associated with bactericidal mechanisms, we next investigated the pathogen-induced expression of iNOS in AMs and BMDMs. Surprisingly, we hereby discovered that PTEN$^{MC\text{-}KO}$ BMDMs stimulated with *S. pneumoniae* expressed significantly higher iNOS levels 8 h postinduction (data not shown), whereas iNOS expression was diminished in PTEN-deficient AMs (Fig. 3*C*). We furthermore confirmed that decreased iNOS expression correlated with suppressed NO production by quantifying nitrite in supernatants of AMs (Fig. 3*C*).

We then isolated primary AMs from PTEN$^{MC\text{-}Wt}$ and PTEN$^{MC\text{-}KO}$ mice and explored their ability to phagocytose *S. pneumoniae* using confocal microscopy as well as an FACS-based phagocytosis assay. By quantifying the proportion of macrophages that contained intracellular bacteria, we discovered a significantly increased uptake of *S. pneumoniae* by PTEN$^{MC\text{-}KO}$ cells ($p < 0.05$ versus wild-type cells) (Fig. 4*A*, 4*B*). Furthermore, performing a killing assay enabled us to demonstrate enhanced bacterial killing by AMs from PTEN$^{MC\text{-}KO}$ mice (Fig. 4*C*).

Hence, these data illustrate that PTEN activity strongly impacted functional properties attributed to macrophages. Although constitutively active PI3K signaling counteracted the proinflammatory TNF-α and iNOS response, it augmented the phagocytic and bactericidal properties of primary AMs upon challenge with *S. pneumoniae* in vitro.

Anti-inflammatory phenotype and reduced neutrophil influx early during pneumococcal pneumonia in PTEN$^{MC\text{-}KO}$ mice

To discern the in vivo impact of myeloid-cell associated PTEN on inflammation during bacterial infection, we then asked how above described findings would translate into the immediate host response during bacterial pneumonia in vivo. For this purpose, we infected PTEN$^{MC\text{-}KO}$ and PTEN$^{MC\text{-}Wt}$ mice with *S. pneumoniae* and studied the early inflammatory response after 6 h. In line with in vitro data depicted in Fig. 3, PTEN$^{MC\text{-}KO}$ animals exhibited a diminished proinflammatory cytokine response, illustrated by significantly lower TNF-α concentrations in BALF of these mice ($p < 0.01$ versus PTEN$^{MC\text{-}Wt}$ mice) (Fig. 5*A*). At the same time, the anti-inflammatory cytokine IL-10 was found significantly increased in lungs of PTEN$^{MC\text{-}KO}$ mice as compared with wild-type animals (Fig. 5*B*), indicating that the constitutive activation of myeloid cell-derived PI3K pathways dampened the inflammatory response in vivo.

Host defense against respiratory tract infections critically depends on the effective influx of neutrophils. Because PI3K activation has been repeatedly shown to promote neutrophil chemotaxis (10), and in light of a recent publication that highlighted the role of myeloid PTEN as a suppressor of neutrophil migration (31), we expected PTEN$^{MC\text{-}KO}$ mice to exhibit an enhanced recruitment of neutrophils to the alveolar compartment. When enumerating the number of cells attracted to the alveolar compartment 6 h postinduction of pneumococcal pneumonia, we surprisingly found a significantly impaired influx of neutrophils in the absence of PTEN (Fig. 5*C*, 5*D*). Despite this reduced neutrophil attraction and diminished TNF-α response, bacterial outgrowth in lungs and BALF of PTEN$^{MC\text{-}KO}$ mice was not affected at this early time point (Fig. 5*E*, 5*F*). Together, PTEN deficiency dampened the early inflammatory response during bacterial pneumonia.

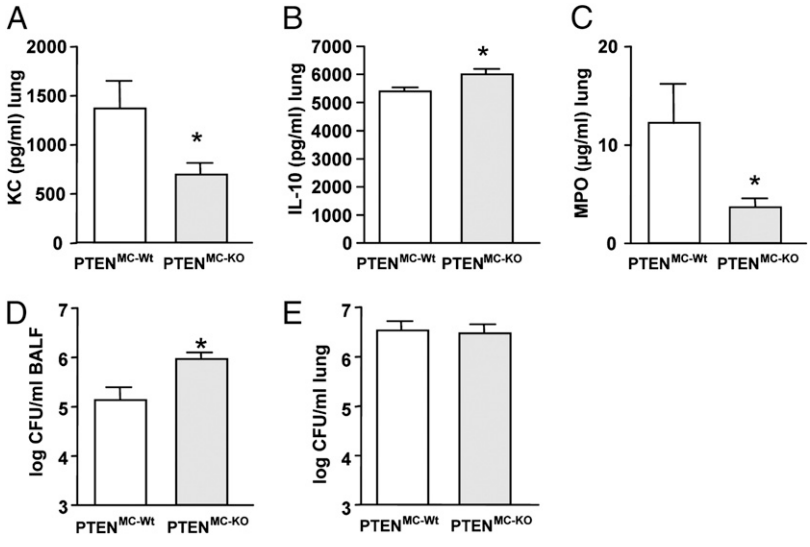

FIGURE 6. Role of PTEN 48 h postinduction of pneumococcal pneumonia. PTEN$^{MC\text{-}KO}$ and littermate PTEN$^{MC\text{-}Wt}$ mice were infected intranasally with 4×10^5 CFU *S. pneumoniae* and sacrificed after 48 h (n = 7–9/group). KC (*A*), IL-10 (*B*), and MPO (*C*) concentrations were determined in lung homogenates by ELISA. Bacterial CFUs were enumerated by plating serial dilutions of BALF (*D*) and lung homogenates (*E*). Data are presented as mean ± SEM. *$p < 0.05$.

Table II. *BALF cellular composition in PTEN$^{MC\text{-}KO}$ and PTEN$^{MC\text{-}Wt}$ mice 48 h post* S. pneumoniae *infection*

BALF	PTEN$^{MC\text{-}Wt}$	PTEN$^{MC\text{-}KO}$
Total cells $\times$ 10^4/ml	11.0 ± 4.6	12.8 ± 7.7
Neutrophils (%)	61.3 ± 5.9	47.7 ± 10.5*
Monocytes/macrophages (%)	38.2 ± 5.8	52.8 ± 10.6*

Data are presented as mean ± SEM of n = 9–10 mice/group.
*$p < 0.05$.

PTEN$^{MC\text{-}KO}$ mice exhibit a diminished inflammatory response and modestly enhanced bacterial burden 48 h postinduction of pneumonia

Having established PTEN's proinflammatory contribution to the induction-phase of *S. pneumoniae* infection in vivo, we then explored PTEN's impact over the course of pneumococcal pneumonia and investigated mice 48 h postinfection. At this later time point, we continued to observe reduced levels of proinflammatory mediators in BALF and lungs of mice lacking PTEN. As depicted in Table I, BALF concentrations of TNF-α, KC, and MCP-1 were significantly decreased, whereas IL-6 showed a modest but nonsignificant reduction in PTEN$^{MC\text{-}KO}$ versus PTEN$^{MC\text{-}Wt}$ mice. In contrast to the alveolar compartment, TNF-α and IL-6 levels did not differ in lung homogenates (data not shown), whereas KC concentrations were considerably decreased, and IL-10 levels significantly increased in lungs from PTEN$^{MC\text{-}KO}$ mice as compared with PTEN$^{MC\text{-}Wt}$ animals (Fig. 6*A*, 6*B*). In line with this diminished chemokine release, PTEN$^{MC\text{-}KO}$ animals displayed an impaired ability to attract neutrophils to the site of infection, as illustrated by a significantly decreased proportion of neutrophils in BALF (Table II) as well as reduced MPO levels in lungs from PTEN$^{MC\text{-}KO}$ mice (Fig. 6*C*) 48 h postinfection. The reduction in proinflammatory mediators and neutrophil influx was accompanied by modestly increased bacterial counts in the alveolar compartment of PTEN$^{MC\text{-}KO}$ mice 48 h postinfection with *S. pneumoniae* (Fig. 6*D*), whereas CFU counts in lung homogenates did not differ between the mouse strains (Fig. 6*E*).

Because PI3K activation has been repeatedly shown to promote migration of neutrophils (7, 8, 21, 32), the continual observation of impaired pulmonary neutrophil recruitment in PTEN$^{MC\text{-}KO}$ mice was unanticipated (Figs. 5*C*, 5*D*, 6*C*). Based on a recent report that illustrated PTEN's suppressive function on neutrophil migration during *Escherichia coli* peritonitis and sterile peritoneal inflammation (31), we wondered whether these contradicting results were due to pathogen- or organ-specific differences that have never been investigated before. To answer this question, we injected *S. pneumoniae* i.p. in PTEN$^{MC\text{-}KO}$ mice and PTEN$^{MC\text{-}Wt}$ littermate controls and enumerated peritoneal neutrophil counts after 6 h. In contrast to the diminished alveolar neutrophil influx during pneumonia, we found an enhanced peritoneal recruitment of neutrophils in animals lacking myeloid cell-associated PTEN (Fig. 7*A*). These findings indicate that organ-specific differences could explain our observation of diminished neutrophil migration in PTEN$^{MC\text{-}KO}$ mice suffering from pneumococcal pneumonia in vivo and argue against a fundamental cellular defect of PTEN-deficient neutrophils. To understand organ-specific differences in more detail, we additionally studied the inflammatory cytokine and chemokine response of primary peritoneal macrophages upon *S. pneumoniae* stimulation in vitro. Comparable to our observations from BMDMs and AMs (Fig. 3), we discovered reduced TNF-α secretion by peritoneal PTEN$^{MC\text{-}KO}$ macrophages (Fig. 7*B*). However, in strong contrast to BMDMs or AMs, peritoneal macrophages that lacked PTEN released significantly more KC than PTEN$^{MC\text{-}Wt}$ cells (Fig. 7*C*). This enhanced chemokine release by PTEN$^{MC\text{-}KO}$ peritoneal macrophages provides a potential explanation for the augmented PMN influx into the peritoneal cavity of PTEN$^{MC\text{-}KO}$ animals.

Constitutively active PI3K does not impact clearance of S. pneumoniae *65 h postinfection*

In an attempt to identify the contributing factors that ultimately led to improved outcome of PTEN$^{MC\text{-}KO}$ mice suffering from pneumococcal pneumonia, we repeated the pneumonia study and sacrificed mice after 65 h (i.e., right before animals started to succumb to infection). We hereby observed significantly decreased IL-6 levels and modestly reduced TNF-α and KC concentrations in BALF of PTEN$^{MC\text{-}KO}$ (Table III). In line with above-described findings at 6 h and 48 h postinfection, we continued to detect significantly higher IL-10 levels in lung homogenates of mice lacking myeloid PTEN (Fig. 8*A*). When analyzing the cellular composition in BALF, we found a predominance of monocytes/macrophages in PTEN$^{MC\text{-}KO}$ mice, whereas neutrophil numbers exceeded monocytes/macrophages in PTEN$^{MC\text{-}Wt}$ littermates (Fig. 8*B*, 8*C*). In accordance, histological evaluation of lung slides disclosed significantly more pronounced signs of inflammation in PTEN$^{MC\text{-}Wt}$ mice than PTEN$^{MC\text{-}KO}$ animals (Fig. 8*F*, 8*G*). However, when enumerating bacterial counts in BALF and lungs, we did not discover any differences between wild-type and PTEN-deficient mice 65 h postinfection (Fig. 8*D*, 8*E*). Furthermore, blood cultures did not reveal any differences between groups (data not shown).

Hence, these data indicate that the continuous activation of PI3K, as seen in PTEN$^{MC\text{-}KO}$ mice, beneficially modulated the inflammatory response to *S. pneumoniae*, thus allowing for accelerated resolution of pneumonia without impairing bacterial clearance in vivo.

Discussion

The role of PI3K pathways in the inflammatory response is a controversial matter, as published reports suggested either proinflammatory or anti-inflammatory properties (15, 33, 34). We and

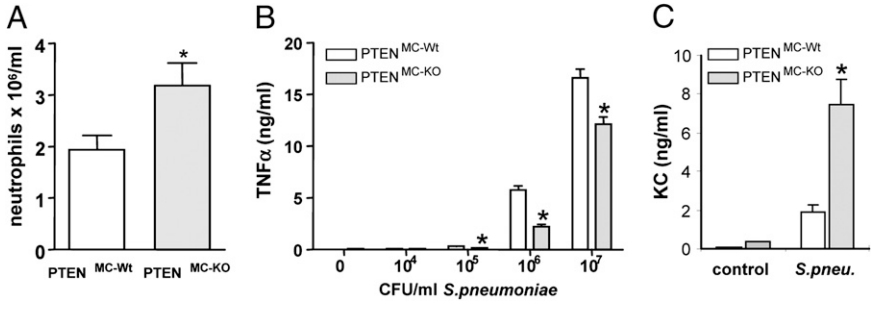

FIGURE 7. Immunomodulatory properties of PTEN during peritoneal inflammation. PTEN$^{MC\text{-}KO}$ and PTEN$^{MC\text{-}Wt}$ littermates were infected i.p. with *S. pneumoniae* (4×10^5 CFU). Peritoneal lavage was performed after 6 h and neutrophils (*A*) were enumerated (n = 6–7 mice/group). Dose-dependent (10^3/ml to 10^7/ml; heat-killed *S. pneumoniae*) TNF-α release (*B*) and KC secretion (*C*) in response to 10^7/ml *S. pneumoniae* was determined in supernatants of PTEN$^{MC\text{-}KO}$ and PTEN$^{MC\text{-}Wt}$ macrophages after 12 h (n = 9 per genotype). Data are presented as mean ± SEM. *$p < 0.05$.

Table III. *BALF cytokine and chemokine levels (pg/ml) in PTEN$^{MC\text{-}KO}$ and PTEN$^{MC\text{-}Wt}$ mice 65 h post* S. pneumoniae *infection*

BALF	PTEN$^{MC\text{-}Wt}$	PTEN$^{MC\text{-}KO}$
TNF-α	201 ± 63	107 ± 35
IL-6	547 ± 115	199 ± 59*
KC	259 ± 114	119 ± 49

Data are presented as mean ± SEM of n = 7–8 mice/group.
*$p < 0.05$.

others demonstrated earlier that PI3K activation exerts protective immunomodulatory effects in murine models of endotoxemia, sepsis, and viral infection (16, 35–37). These findings have been partly attributed to PI3K's ability to modulate the transcriptional activity of NF-κB and to efficiently limit proinflammatory signaling cascades induced via MAPK pathways (11, 34). Given that PTEN is a key regulator of PI3K activity, we hypothesized that PTEN might act as a critical modulator of the inflammatory response during bacterial infection. To investigate this idea in a clinically relevant model, we studied the role of PTEN during *S. pneumoniae* pneumonia in vivo and discovered that myeloid cell-specific PTEN deficiency exerted beneficial effects. PTEN deficiency was associated with diminished TNF-α and increased IL-10 responses, enhanced macrophage phagocytosis, reduced neutrophil migration to lungs, and, ultimately, improved survival.

Modulation of PI3K activity by cell type-specific *pten* gene ablation disclosed a markedly reduced TNF-α response by various primary macrophage subsets that were stimulated with *S. pneumoniae*. These findings correlated with earlier observations by us and other investigators who showed that LPS-challenged PTEN-deficient macrophages displayed a profoundly reduced TNF-α release and diminished activation of MAPKs (15, 38). We concurrently discovered the enhanced phosphorylation of GSK3β in PTEN-deficient macrophages. GSK3β is a constitutively active serine/threonine kinase and downstream target of PI3K that can be inactivated through phosphorylation by Akt (39). The biological significance of GSK3β during inflammation was discovered by Martin et al. (16), who revealed that GSK3β inhibition led to a diminished inflammatory response toward various TLR agonists, which was illustrated by reduced TNF-α and enhanced IL-10 releases. In striking agreement with this report, we hereby observed decreased levels of proinflammatory cytokines, such as TNF-α and elevated concentrations of the anti-inflammatory cytokine IL-10 in lungs of *S. pneumoniae*-infected PTEN$^{MC\text{-}KO}$ animals. Therefore, enhanced phosphorylation and consecutive inactivation of GSK3β activity in macrophages of PTEN$^{MC\text{-}KO}$ animals might explain our in vivo findings of a dampened inflammatory response in these mice.

The most unanticipated finding of our studies was the diminished pulmonary neutrophil influx in PTEN$^{MC\text{-}KO}$ mice suffering from pneumococcal pneumonia. Importantly, this observation was not related to constitutively reduced neutrophil numbers in

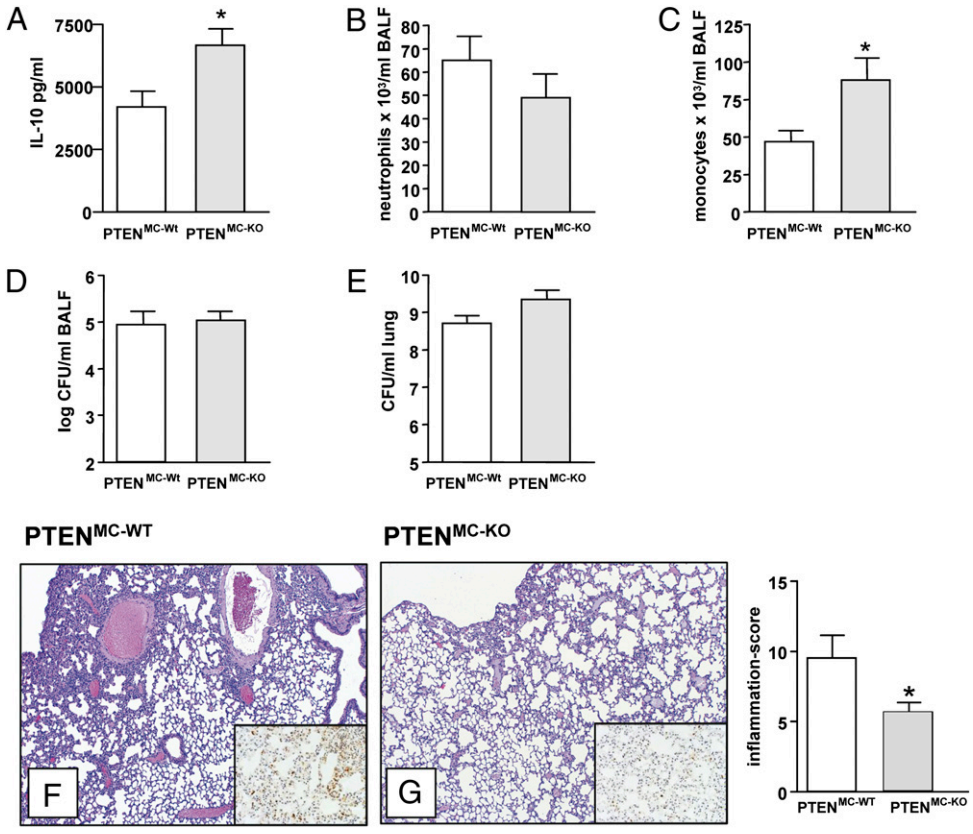

FIGURE 8. Unaltered bacterial counts despite reduced inflammation in PTEN$^{MC\text{-}KO}$ mice 65 h postinfection. PTEN$^{MC\text{-}KO}$ and PTEN$^{MC\text{-}Wt}$ littermates were infected with 4×10^5 CFU *S. pneumoniae* and sacrificed after 65 h. *A*, Whole lung IL-10 concentrations were determined by ELISA. Neutrophil (*B*) and monocyte/macrophage (*C*) influx into the bronchoalveolar compartment was determined on cytospins. Bacterial CFUs in BALF (*D*) and lungs (*E*) were quantified by plating serial dilutions on blood agar plates. *F* and *G*, Representative lung histology images of PTEN$^{MC\text{-}Wt}$ and PTEN$^{MC\text{-}KO}$ mice 65 h postinfection. Lung sections stained with H&E were scored (as described in the *Materials and Methods* section) by a trained pathologist blinded for groups and are expressed as inflammation score. The insets are representative pictures of immunostaining for neutrophils, confirming reduced influx in PTEN$^{MC\text{-}KO}$ mice. *F* and *G*, H&E, original magnification ×4; inset, Ly6-staining, original magnification ×20. Data are presented as mean ± SEM of n = 7–8 mice/group. *$p < 0.05$.

this specific mouse strain, because we previously showed that blood neutrophil numbers were even higher in healthy PTEN$^{MC\text{-}KO}$ animals as compared with wild-type mice (15). In support of the general notion of PI3K being a key player in cell migration (6–8, 10, 19), the migratory capacity of PTEN-deficient neutrophils was found enhanced in earlier reports (31). Furthermore, increased neutrophil recruitment was observed in PTEN$^{MC\text{-}KO}$ animals using models of thioglycollate or *E. coli*-induced peritonitis in vivo (31). Although we were able to confirm these data, as we also observed enhanced peritoneal neutrophil influx following thioglycollate administration in PTEN$^{MC\text{-}KO}$ mice (data not shown), we consistently observed reduced alveolar neutrophil migration during pneumococcal pneumonia in PTEN$^{MC\text{-}KO}$ animals. To exclude the possibility of pathogen-specific differences, we challenged mice i.p. with *S. pneumoniae* and observed enhanced peritoneal neutrophil recruitment in PTEN$^{MC\text{-}KO}$ mice (Fig. 7*A*). Because neutrophil attraction to sites of infection critically depends on the effective release of chemokines, such as KC (40, 41), we investigated if organ-specific differences in neutrophil migration in PTEN$^{MC\text{-}KO}$ animals were a consequence of altered chemokine release by resident macrophages. Indeed, when measuring KC concentrations in supernatants of alveolar and peritoneal macrophages that were stimulated with *S. pneumoniae* in vitro, we discovered an enhanced KC release by peritoneal but not alveolar PTEN$^{MC\text{-}KO}$ macrophages. Beside macrophages, respiratory epithelial cells are a major source of KC within the lungs in vivo, and release of this chemokine is largely triggered by macrophage-derived proinflammatory cytokines, such as TNF-α (42). The fact that we identified reduced KC levels in lung-homogenates from infected PTEN$^{MC\text{-}KO}$ mice in vivo (Table I) might therefore result from the attenuated macrophage-associated (e.g., TNF-α–mediated) activation of airway epithelial cells in vivo, ultimately resulting in reduced neutrophil recruitment. In contrast to our observations, Li et al. (43) disclosed increased pulmonary KC concentrations and enhanced neutrophil migration in PTEN-deficient mice suffering from *E. coli* pneumonia. It therefore seems that PTEN differentially regulates the attraction of neutrophils depending on either the affected organ and/or the inducing agent.

Unlike neutrophils, cells of monocytic origin (infiltrating monocytes/macrophages) were recruited in increased numbers to lungs of healthy and *S. pneumoniae*-infected PTEN$^{MC\text{-}KO}$ mice (data not shown) (Table I). This result is in agreement with a report by Maus et al. (17), who showed that monocyte/macrophage recruitment in pneumoccocal pneumonia critically depended on proper p110γ signal transduction. We recently demonstrated that AMs crucially contribute to host defense during murine pneumococcal pneumonia, as they exert an important role in the resolution of pneumococcal pneumonia by virtue of their capacity to eliminate apoptotic neutrophils (29). This idea is strengthened by data obtained in p110γ-deficient mice in which the recruitment of monocytes/macrophages was found to be impaired (17 and data not shown). PI3Kγ-KO mice showed substantial lung infiltrates and tissue injury during pneumococcal pneumonia (data not shown), whereas PTEN$^{MC\text{-}KO}$ mice that embraced significantly increased numbers of (alveolar) macrophages showed less severe signs of tissue damage (Fig. 8). We in addition discovered an increased phagocytic and killing potential of AMs in the absence of PTEN. The enhanced phagocytic properties of PTEN-deficient macrophages might have compensated for the reduced number of infiltrating neutrophils. However, the precise role of neutrophils during pneumococcal pneumonia has been challenged recently by a report showing unaltered bacterial clearance and improved survival in neutrophil-depleted animals that were infected with *S. pneumoniae* (44). It seems that enhanced neutrophil numbers prolong inflammation and ultimately fuel tissue damage, thus resulting in worsened outcome. It is therefore tempting to hypothesize that lower neutrophil counts and simultaneously increased numbers of macrophages in PTEN$^{MC\text{-}KO}$ animals improved bacterial clearance and augmented the resolution of inflammation, thus contributing to diminished tissue damage and favorable outcome in these animals.

In conclusion, our findings demonstrate that enhanced PI3K activity in PTEN-deficient mice resulted in an improved outcome during pneumococcal pneumonia. These findings implicate a crucial role for PTEN in the homeostasis of pro- and anti-inflammatory mechanisms evoked during a relevant bacterial infection. Thus, interfering with PI3K signaling might have tremendous implications on the course of pneumococcal pneumonia: although blockade of PTEN might be beneficial, reduced PI3K activity might prove detrimental.

Acknowledgments

We thank L. Erhart and R. Raim for excellent technical assistance.

Disclosures

The authors have no financial conflicts of interest.

References

1. National Immunization Program. 2007. *Epidemiology and Prevention of Vaccine-Preventable Diseases.* Centers for Disease Control and Prevention and U.S. Department of Health and Human Services, Atlanta, GA.
2. Ortqvist, A., J. Hedlund, and M. Kalin. 2005. *Streptococcus pneumoniae*: epidemiology, risk factors, and clinical features. *Semin. Respir. Crit. Care Med.* 26: 563–574.
3. Appelbaum, P. C. 2002. Resistance among *Streptococcus pneumoniae*: Implications for drug selection. *Clin. Infect. Dis.* 34: 1613–1620.
4. Tamguney, T., and D. Stokoe. 2007. New insights into PTEN. *J. Cell Sci.* 120: 4071–4079.
5. Cantley, L. C. 2002. The phosphoinositide 3-kinase pathway. *Science* 296: 1655–1657.
6. Curnock, A. P., M. K. Logan, and S. G. Ward. 2002. Chemokine signalling: pivoting around multiple phosphoinositide 3-kinases. *Immunology* 105: 125–136.
7. Hirsch, E., V. L. Katanaev, C. Garlanda, O. Azzolino, L. Pirola, L. Silengo, S. Sozzani, A. Mantovani, F. Altruda, and M. P. Wymann. 2000. Central role for G protein-coupled phosphoinositide 3-kinase gamma in inflammation. *Science* 287: 1049–1053.
8. Li, Z., H. Jiang, W. Xie, Z. Zhang, A. V. Smrcka, and D. Wu. 2000. Roles of PLC-beta2 and -beta3 and PI3Kgamma in chemoattractant-mediated signal transduction. *Science* 287: 1046–1049.
9. Sasaki, T., J. Irie-Sasaki, R. G. Jones, A. J. Oliveira-dos-Santos, W. L. Stanford, B. Bolon, A. Wakeham, A. Itie, D. Bouchard, I. Kozieradzki, et al. 2000. Function of PI3Kgamma in thymocyte development, T cell activation, and neutrophil migration. *Science* 287: 1040–1046.
10. Stephens, L., C. Ellson, and P. Hawkins. 2002. Roles of PI3Ks in leukocyte chemotaxis and phagocytosis. *Curr. Opin. Cell Biol.* 14: 203–213.
11. Fukao, T., and S. Koyasu. 2003. PI3K and negative regulation of TLR signaling. *Trends Immunol.* 24: 358–363.
12. Ruse, M., and U. G. Knaus. 2006. New players in TLR-mediated innate immunity: PI3K and small Rho GTPases. *Immunol. Res.* 34: 33–48.
13. Guha, M., and N. Mackman. 2002. The phosphatidylinositol 3-kinase-Akt pathway limits lipopolysaccharide activation of signaling pathways and expression of inflammatory mediators in human monocytic cells. *J. Biol. Chem.* 277: 32124–32132.
14. Günzl, P., and G. Schabbauer. 2008. Recent advances in the genetic analysis of PTEN and PI3K innate immune properties. *Immunobiology* 213: 759–765.
15. Luyendyk, J. P., G. A. Schabbauer, M. Tencati, T. Holscher, R. Pawlinski, and N. Mackman. 2008. Genetic analysis of the role of the PI3K-Akt pathway in lipopolysaccharide-induced cytokine and tissue factor gene expression in monocytes/macrophages. *J. Immunol.* 180: 4218–4226.
16. Martin, M., K. Rehani, R. S. Jope, and S. M. Michalek. 2005. Toll-like receptor-mediated cytokine production is differentially regulated by glycogen synthase kinase 3. *Nat. Immunol.* 6: 777–784.
17. Maus, U. A., M. Backi, C. Winter, M. Srivastava, M. K. Schwarz, T. Rückle, J. C. Paton, D. Briles, M. Mack, T. Welte, et al. 2007. Importance of phosphoinositide 3-kinase gamma in the host defense against pneumococcal infection. *Am. J. Respir. Crit. Care Med.* 175: 958–966.
18. Marone, R., V. Cmiljanovic, B. Giese, and M. P. Wymann. 2008. Targeting phosphoinositide 3-kinase: moving towards therapy. *Biochim. Biophys. Acta* 1784: 159–185.
19. Suzuki, A., M. T. Yamaguchi, T. Ohteki, T. Sasaki, T. Kaisho, Y. Kimura, R. Yoshida, A. Wakeham, T. Higuchi, M. Fukumoto, et al. 2001. T cell-specific loss of Pten leads to defects in central and peripheral tolerance. *Immunity* 14: 523–534.

20. Peyssonnaux, C., V. Datta, T. Cramer, A. Doedens, E. A. Theodorakis, R. L. Gallo, N. Hurtado-Ziola, V. Nizet, and R. S. Johnson. 2005. HIF-1alpha expression regulates the bactericidal capacity of phagocytes. *J. Clin. Invest.* 115: 1806–1815.
21. Davies, J. Q., and S. Gordon. 2005. Isolation and culture of murine macrophages. *Methods Mol. Biol.* 290: 91–103.
22. Knapp, S., S. Florquin, D. T. Golenbock, and T. van der Poll. 2006. Pulmonary lipopolysaccharide (LPS)-binding protein inhibits the LPS-induced lung inflammation in vivo. *J. Immunol.* 176: 3189–3195.
23. Lagler, H., O. Sharif, I. Haslinger, U. Matt, K. Stich, T. Furtner, B. Doninger, K. Schmid, R. Gattringer, A. F. de Vos, and S. Knapp. 2009. TREM-1 activation alters the dynamics of pulmonary IRAK-M expression in vivo and improves host defense during pneumococcal pneumonia. *J. Immunol.* 183: 2027–2036.
24. LeBel, C. P., H. Ischiropoulos, and S. C. Bondy. 1992. Evaluation of the probe 2′,7′-dichlorofluorescin as an indicator of reactive oxygen species formation and oxidative stress. *Chem. Res. Toxicol.* 5: 227–231.
25. Knapp, S., U. Matt, N. Leitinger, and T. van der Poll. 2007. Oxidized phospholipids inhibit phagocytosis and impair outcome in gram-negative sepsis in vivo. *J. Immunol.* 178: 993–1001.
26. Knapp, S., L. Hareng, A. W. Rijneveld, P. Bresser, J. S. van der Zee, S. Florquin, T. Hartung, and T. van der Poll. 2004. Activation of neutrophils and inhibition of the proinflammatory cytokine response by endogenous granulocyte colony-stimulating factor in murine pneumococcal pneumonia. *J. Infect. Dis.* 189: 1506–1515.
27. Knapp, S., C. W. Wieland, C. van 't Veer, O. Takeuchi, S. Akira, S. Florquin, and T. van der Poll. 2004. Toll-like receptor 2 plays a role in the early inflammatory response to murine pneumococcal pneumonia but does not contribute to antibacterial defense. *J. Immunol.* 172: 3132–3138.
28. Knapp, S., J. C. Leemans, S. Florquin, J. Branger, N. A. Maris, J. Pater, N. van Rooijen, and T. van der Poll. 2003. Alveolar macrophages have a protective antiinflammatory role during murine pneumococcal pneumonia. *Am. J. Respir. Crit. Care Med.* 167: 171–179.
29. Dessing, M. C., S. Knapp, S. Florquin, A. F. de Vos, and T. van der Poll. 2007. CD14 facilitates invasive respiratory tract infection by *Streptococcus pneumoniae*. *Am. J. Respir. Crit. Care Med.* 175: 604–611.
30. Sly, L. M., V. Ho, F. Antignano, J. Ruschmann, M. Hamilton, V. Lam, M. J. Rauh, and G. Krystal. 2007. The role of SHIP in macrophages. *Front. Biosci.* 12: 2836–2848.
31. Subramanian, K. K., Y. Jia, D. Zhu, B. T. Simms, H. Jo, H. Hattori, J. You, J. P. Mizgerd, and H. R. Luo. 2007. Tumor suppressor PTEN is a physiologic suppressor of chemoattractant-mediated neutrophil functions. *Blood* 109: 4028–4037.
32. Liu, L., K. D. Puri, J. M. Penninger, and P. Kubes. 2007. Leukocyte PI3Kgamma and PI3Kdelta have temporally distinct roles for leukocyte recruitment in vivo. *Blood* 110: 1191–1198.
33. Strassheim, D., J. Y. Kim, J. S. Park, S. Mitra, and E. Abraham. 2005. Involvement of SHIP in TLR2-induced neutrophil activation and acute lung injury. *J. Immunol.* 174: 8064–8071.
34. Hazeki, K., K. Nigorikawa, and O. Hazeki. 2007. Role of phosphoinositide 3-kinase in innate immunity. *Biol. Pharm. Bull.* 30: 1617–1623.
35. Williams, D. L., C. Li, T. Ha, T. Ozment-Skelton, J. H. Kalbfleisch, J. Preiszner, L. Brooks, K. Breuel, and J. B. Schweitzer. 2004. Modulation of the phosphoinositide 3-kinase pathway alters innate resistance to polymicrobial sepsis. *J. Immunol.* 172: 449–456.
36. Schabbauer, G., M. Tencati, B. Pedersen, R. Pawlinski, and N. Mackman. 2004. PI3K-Akt pathway suppresses coagulation and inflammation in endotoxemic mice. *Arterioscler. Thromb. Vasc. Biol.* 24: 1963–1969.
37. Schabbauer, G., J. Luyendyk, K. Crozat, Z. Jiang, N. Mackman, S. Bahram, and P. Georgel. 2008. TLR4/CD14-mediated PI3K activation is an essential component of interferon-dependent VSV resistance in macrophages. *Mol. Immunol.* 45: 2790–2796.
38. Cao, X., G. Wei, H. Fang, J. Guo, M. Weinstein, C. B. Marsh, M. C. Ostrowski, and S. Tridandapani. 2004. The inositol 3-phosphatase PTEN negatively regulates Fc gamma receptor signaling, but supports Toll-like receptor 4 signaling in murine peritoneal macrophages. *J. Immunol.* 172: 4851–4857.
39. Doble, B. W., and J. R. Woodgett. 2003. GSK-3: tricks of the trade for a multitasking kinase. *J. Cell Sci.* 116: 1175–1186.
40. Fillion, I., N. Ouellet, M. Simard, Y. Bergeron, S. Sato, and M. G. Bergeron. 2001. Role of chemokines and formyl peptides in pneumococcal pneumonia-induced monocyte/macrophage recruitment. *J. Immunol.* 166: 7353–7361.
41. Frevert, C. W., S. Huang, H. Danaee, J. D. Paulauskis, and L. Kobzik. 1995. Functional characterization of the rat chemokine KC and its importance in neutrophil recruitment in a rat model of pulmonary inflammation. *J. Immunol.* 154: 335–344.
42. Jones, M. R., B. T. Simms, M. M. Lupa, M. S. Kogan, and J. P. Mizgerd. 2005. Lung NF-kappaB activation and neutrophil recruitment require IL-1 and TNF receptor signaling during pneumococcal pneumonia. *J. Immunol.* 175: 7530–7535.
43. Li, Y., Y. Jia, M. Pichavant, F. Loison, B. Sarraj, A. Kasorn, J. You, B. E. Robson, D. T. Umetsu, J. P. Mizgerd, et al. 2009. Targeted deletion of tumor suppressor PTEN augments neutrophil function and enhances host defense in neutropenia-associated pneumonia. *Blood* 113: 4930–4941.
44. Marks, M., T. Burns, M. Abadi, B. Seyoum, J. Thornton, E. Tuomanen, and L. A. Pirofski. 2007. Influence of neutropenia on the course of serotype 8 pneumococcal pneumonia in mice. *Infect. Immun.* 75: 1586–1597.